

Effective minimal model and unconventional spin-singlet pairing in Kagome superconductor CsV_3Sb_5

Xiao-Cheng Bai*, Wen-Feng Wu*, Han-Yu Wang, Ya-Min Quan, Xian-Long Wang, Zhi Zeng,[†] and Liang-Jian Zou[‡]

¹ Key Laboratory of Materials Physics,
Institute of Solid State Physics, HFIPS,

Chinese Academy of Sciences, Hefei 230031, China

² Science Island Branch of Graduate School,
University of Science and Technology of China, Hefei 230026, China

(Dated: today)

Recently synthesized Kagome compounds AV_3Sb_5 attract great attention due to the unusual coexistence of the topology, charge density wave and superconductivity. In this *Letter*, based on the band structures for CsV_3Sb_5 in pristine phase, we fit an effective 6-band model for the low-energy processes; utilizing the random phase approximation (RPA) on the effective minimal model, we obtain the momentum-resolved dynamical spin susceptibility; attributing the spin-fluctuation pairing mechanism, we find that the superconducting pairing strengths increase with the lift of the Coulomb correlation, and the superconductive pairing symmetry is singlet, most probably with the d_{xy} symmetry in the intermediate to strong Coulomb correlated regime, indicating the unconventional superconductivity in Kagome compounds AV_3Sb_5 .

PACS numbers:

Introduction: Local spins in a Kagome lattice compound was regarded as most probably forming exotic quantum spin liquid^{1,2}. Once such Kagome compounds³ become superconductive⁴⁻¹⁸, the long-term searching relationship between quantum spin liquid phase and unconventional superconductivity seems link with each other; recently found novel Kagome lattice compounds AV_3Sb_5 ($A=\text{K}, \text{Rb}, \text{Cs}$) have been attracting great research interest⁴⁻²⁷. Through recent great efforts, many physical properties of AV_3Sb_5 , including the electronic structures^{3,19-22}, normal-state^{3,24} and superconducting-state properties⁴⁻¹⁸, pressure effect⁷⁻¹⁰, magnetic field effect¹¹⁻¹³, STM results¹⁴⁻¹⁶ and ARPES data²⁵⁻²⁷ have gradually become clear. Several theoretical models were also proposed^{28,29} to address the chirality of the charge-density-wave state and superconductivity. Nevertheless, a few of essential features remain not revealed, including the effective low-energy model, superconducting pairing force and the pairing symmetry, *etc.*

Due to unique crystal structure of Kagome compounds AV_3Sb_5 , the electronic structures of normal-state AV_3Sb_5 are rather complicated. The band structures of the pristine phase of CsV_3Sb_5 ¹⁹, calculated by the density functional theory (DFT), predicted that seven bands cross the Fermi energy E_F and are composed of V 3d orbitals and Sb 5p orbitals, which shows typical multi-orbital character. Since the unit cell of Kagome lattice contains three V sites in the pristine phase, at the same time, the metallic ground state in AV_3Sb_5 and partial filled V 3d orbitals also imply the multi-orbital character in the low-energy model. These inevitably bring difficulty in constructing an effective multi-orbital model for superconducting AV_3Sb_5 . At present the microscopic origin of the charge density wave is generally attributed to the *van Hove* singularity, whereas, to understand the essential superconductive nature, a proper effective model correctly

describing the low-energy processes plays key roles and is highly expected.

So-far experimental data strongly support unconventional superconductive pairing mechanism in AV_3Sb_5 : conventional e-ph coupling mechanism is not enough to account for the superconductive microscopic origin, neither the transition temperatures estimated by the McMillan's formula for RbV_3Sb_5 and CsV_3Sb_5 considerably deviate from the experimental T_C ¹⁹, nor the experimental T_c violates the expectation of the conventional e-ph mechanism when A varies from K, Rb to Cs. AV_3Sb_5 superconductors also display many features of unconventional superconductivity: with the increase of hydrostatic pressure, the P-T phase diagram demonstrates two superconductive regions^{7,10}, similar to the two-dome superconductive phase diagrams in iron-based superconductors^{30,31}. Though the local magnetic moment was argued to be absent³², the observation of the anomalous Hall effect in CsV_3Sb_5 ³³ strongly favors of the presence of local magnetic field, hence the local spins. The first-principles electronic structure calculations also suggested there exists local magnetic moments in AV_3Sb_5 ^{20,21}, implying that the spin-orbital fluctuations mechanism is the possible pairing origin, since not only the system possesses local magnetic moments and multiorbital character, but also Kagome lattice structure favors strong spin frustrations and fluctuations. These eager further deep theoretical investigations.

On the other hand, the details of the superconductive nature in AV_3Sb_5 are not clear. A very recent study²⁹ suggested that the superconducting electrons in CsV_3Sb_5 are f-wave triplet pairing: *i.e.* the superconductive Cooper pairs are spatial f-wave, and spin parallel or triplet. On a contrast, in similar sixfold-symmetric superconductor $\text{Na}_x\text{CoO}_2\cdot y\text{H}_2\text{O}$, an earlier theoretical investigation suggested to be f-wave

pairing symmetry³⁴, however, the experiments supported that the pairing symmetry of superconducting cobaltates is singlet d-wave³⁵. This arises the puzzle whether the Cooper pairs with high angular momentum could stably exist in AV_3Sb_5 . In this Letter, based on our calculated band structures for CsV_3Sb_5 in the pristine phase, we fit an effective low-energy 6-band model; utilizing the random phase approximation (RPA) on the effective minimal model, we show that the superconducting pairing strengths increase with the increase of Coulomb correlation, and the superconductive pairing symmetry is singlet d_{xy} -wave. The present theoretical results favor our understand on the unconventional superconductivity in Kagome compounds AV_3Sb_5 .

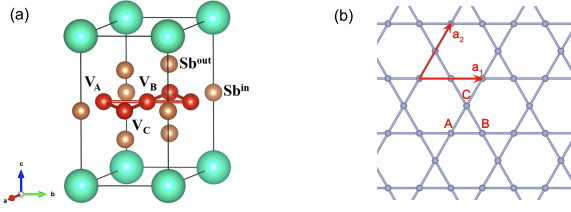


FIG. 1: (a) The crystal structure of pristine phase CsV_3Sb_5 . Red, yellow and green balls represent V, Sb and Cs. Sb^{in} and Sb^{out} indicate that Sb is in the same plane as V and out of the V-Sb plane, respectively. (b) The basic vectors and different V sites on the Kagome plane.

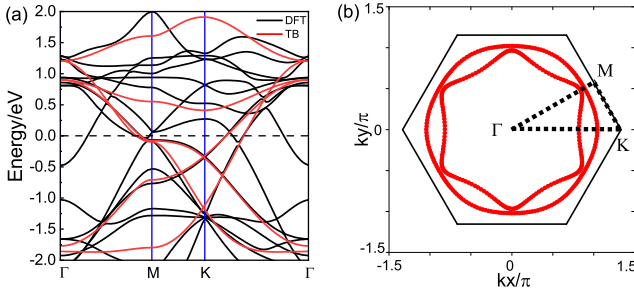


FIG. 2: (a) The band structures of pristine CsV_3Sb_5 (black lines) and fitting by six-band tight-binding model (red lines); (b) Fermi surface of the six band tight-binding model.

Effective minimal model Hamiltonian: To investigate the many body effects and superconductivity in AV_3Sb_5 , one should first construct an effective low-energy model. To this end, we start to perform the first-principles electronic structures calculations to obtain the band structures of CsV_3Sb_5 . The details of the method and the calculations are given in the *Supplementary Materials*. Fig.1(a) shows the crystal structure of the layered CsV_3Sb_5 . Recent resistivity measurement on CsV_3Sb_5 ⁴ showed remarkable anisotropy of the ab -plane to the c -axis, indicating that the interlayer V-V hybridization is rather small. Throughout this paper we confine our study on the V-Sb Kagome plane, as seen in Fig.1(b).

Through orbital analysis to the band structures of CsV_3Sb_5 shown in Fig.2(a), we find that there are three distinct Fermi surface sheets at $k_z=0$: (i) a central ring sheet around Γ contributed by Sb- p_z orbitals, (ii) a hexagonal sheet composed of V- d_{xy} , V- $d_{x^2-y^2}$, and V- d_{z^2} , and (iii) two additional sheets composed of V- d_{xz}/d_{yz} orbitals. The band structures and Fermi surfaces are in agreement with available literature.^{22,23}. By constructing localized Wannier functions, the hopping integrals between different V orbitals α and β ($\alpha = xz, yz$, $\beta = xy, 3z^2 - r^2, x^2 - y^2$) are zeros, see the TABLE S1 in *Supplementary Materials*, indicating that interorbital hybridization between vanadiums is vanishing small, so we neglect the interorbital hopping terms in the tight-binding model. In fitting the band structures with an effective low-energy tight-binding model, we consider the large hexagonal Fermi pocket (ii) and one of the Fermi surface sheets (iii), to which the corresponding energy bands are hybridized weakly with the p orbitals of Sb²², and then construct a six-band tight-binding (TB) model with two local orbitals on each V site. The fitted tight-binding bands and the full electronic structures of CsV_3Sb_5 are the red and black lines in Fig.2(a), respectively.

The fitted six pack-band tight-binding model for CsV_3Sb_5 can be written as

$$H_{TB} = \sum_{k,i,j,\alpha,\sigma} \xi_{ij,\alpha}(k) c_{k,i\alpha\sigma}^\dagger c_{k,j\alpha\sigma} \quad (1)$$

where the inequivalent V sites $i, j = A, B, C$, the orbital indices $\alpha, \beta = 1, 2$, and the hopping matrix elements $\xi_{ij,\alpha}(k) = [(\varepsilon_\alpha + t''_\alpha \phi^3(k) - \mu) \delta_{ij} + t_\alpha \phi_{ij}^1(k) + t'_\alpha \phi_{ij}^2(k)]$, where ϕ^n denotes the lattice structure factor defined in *Supplementary Materials*. The ε_α denotes the energy level of the orbital α and μ is the chemical potential. The operator $c_{k,i,\alpha\sigma}^\dagger$ ($c_{k,i,\alpha\sigma}$) creates (annihilates) an electron with momentum k and spin σ of sublattice i in orbital α . The t_α , t'_α and t''_α denote intra-orbital hopping integrals for the first, second and third nearest neighbors respectively. The hopping parameters and lattice structure factors are given in *Supplementary Materials*, see TABLE S3. Within the present six-band model, the Fermi surface is plotted in Fig.2(b). The corresponding electron filling number is $n=5.69$ to match the chemical potential of CsV_3Sb_5 .

To investigate the spin fluctuations and superconducting pairing properties in CsV_3Sb_5 , we consider the on-site Coulomb interaction as following

$$H_{int} = U \sum_{li,\alpha} n_{li\alpha\uparrow} n_{li\alpha\downarrow} + \sum_{li,\sigma,\sigma',\alpha>\beta} U' n_{li\alpha\sigma} n_{li\beta\sigma'} - J_H \sum_{li,\alpha>\beta} c_{li\alpha\uparrow}^\dagger c_{li\alpha\downarrow} c_{li\beta\downarrow}^\dagger c_{li\beta\uparrow} + J_P \sum_{li,\alpha\neq\beta} c_{li\alpha\uparrow}^\dagger c_{li\alpha\downarrow} c_{li\beta\downarrow}^\dagger c_{li\beta\uparrow}, \quad (2)$$

here l denote the l -th unit cell. The on-site intra- and interorbital Coulomb repulsions are denoted by U and U' .

J_H and J_P are the Hund's rule exchange and pair-hopping term, respectively. Throughout this paper, we set the Coulomb and Hund's interaction parameters $U' = U - 2J_H$ and $J_H = J_P = U/8$, which satisfy spin rotational invariance. The fact that the DFT band structures are in good agreement with the angle-resolved photoemission spectroscopy (ARPES) data⁴, demonstrates that the electronic correlation in CsV_3Sb_5 is not very strong.

Within the random phase approximation (RPA), the singlet (s) and triplet (t) pairing vertices arising from spin and charge fluctuations for the multiorbital case^{36,37} are given by

$$\begin{aligned} \Gamma_{st}^{pq,s}(k, k', \omega) = & \left[\frac{3}{2} U^s \chi_S^{RPA}(k - k', \omega) U^s \right. \\ & \left. - \frac{1}{2} U^c \chi_O^{RPA}(k - k', \omega) U^c + \frac{1}{2} (U^s + U^c) \right]_{ps}^{qt}, \end{aligned} \quad (3)$$

$$\begin{aligned} \Gamma_{st}^{pq,t}(k, k', \omega) = & \left[-\frac{1}{2} U^s \chi_S^{RPA}(k - k', \omega) U^s \right. \\ & \left. - \frac{1}{2} U^c \chi_O^{RPA}(k - k', \omega) U^c + \frac{1}{2} (U^s + U^c) \right]_{ps}^{qt}, \end{aligned} \quad (4)$$

here U^s and U^c represent the 12×12 matrices in the V orbital space, and χ_S^{RPA} and χ_O^{RPA} are the ones RPA spin and orbital (charge) susceptibility matrix given in the Sec. III of *Supplementary Materials*.

By projecting the zero frequency ($\omega = 0$) pairing vertex into the band space^{38,39}, we obtain

$$\begin{aligned} \Gamma_{i,j}^{s/t}(k, k') = & \sum_{s,t,p,q} a_i^{s,*}(k) a_i^{t,*}(-k) \text{Re} \left[\Gamma_{st}^{pq,s/t}(k, k', 0) \right] \\ & \times a_j^p(k') a_j^q(-k'). \end{aligned} \quad (5)$$

The $\Gamma_{i,j}^s(k, k')$ (or $\Gamma_{i,j}^t(k, k')$) determines the scatterings of two electrons of opposite (or same) spin from the state $(k, -k)$ on the Fermi surface sheet C_i to the state $(k', -k')$ on the Fermi surface sheet C_j . By means of a mean-field decoupling of the interaction, the gap equation in singlet and triplet channels can be obtained and expressed as

$$\Delta_k^{i,s/t} = -\frac{1}{2N} \sum_{j,k'} V_{i,j}^{s/t}(k, k') \frac{\Delta_{k'}^{j,s/t}}{\Omega_{k'}^{j,s/t}} \tanh\left(\frac{\beta \Omega_{k'}^{j,s/t}}{2}\right) \quad (6)$$

with

$$\Omega_k^{i,s/t} = \sqrt{[E_i(k)]^2 + |\Delta_k^{i,s/t}|^2}, \quad (7)$$

$$V_{i,j}^s(k, k') = \frac{1}{2} [\Gamma_{i,j}^s(k, k') + \Gamma_{i,j}^s(-k, k')], \quad (8)$$

$$V_{i,j}^t(k, k') = \frac{1}{2} [\Gamma_{i,j}^t(k, k') - \Gamma_{i,j}^t(-k, k')]. \quad (9)$$

It is worthy noting that $\Delta_k^{i,s}$ is an even function with respect to \mathbf{k} and $\Delta_k^{i,t}$ an odd function. The superconducting instability appears at temperature. When the temperature just below

T_c the gap function $\Delta_k^{i,s/t}$ are expected to be very small, and hence we study the superconducting instability by solving the linearized gap equations^{38,40}

$$-\frac{1}{V_G} \sum_j \oint \frac{dk'}{|v_{F_j}(k')|} V_{i,j}^{s/t}(k, k') g_j^\alpha(k') = \lambda_\alpha g_i^\alpha(k). \quad (10)$$

Here the eigenvalues λ_α are the superconducting pairing strengths and $g_i^\alpha(k)$ the corresponding eigenfunctions. V_G is the area of a Brillouin zone, i and j are the band indices of Fermi surface vectors k, k' , respectively, $|v_{F_j}(k')|$ is the magnitude of the Fermi velocity. The largest pairing strength λ_α determines the highest transition temperature and the corresponding eigenfunction $g_i^\alpha(k)$ shows the symmetry of the gap function. Throughout this paper we perform the calculations at temperature of $k_B T = 0.002$ eV.

Momentum-resolved Spin Susceptibility: The distribution of spin susceptibility in momentum space may not only disclose the spin fluctuation modes or the magnetic order, but also provide the superconductive pairing information. The RPA spin susceptibility of the effective minimal model for pristine CsV_3Sb_5 shows six peaks near $\mathbf{q}_1 \approx \frac{1}{4}\Gamma K$ and other five sixfold-symmetric wavevectors, as seen the red points in Fig. 3(a). In the lines connecting these maxima, the magnitude of the spin susceptibility is also very large, as seen the yellow lines in Fig. 3(a). These indicate that there exist multi-mode antiferromagnetic spin fluctuations. We also find that these peaks are enhanced with the increase of the Coulomb correlation U or the decline of the temperature, as seen in 3(b) and Fid.S3 in *Supplementary Materials*.

Note that the e-ph coupling mechanism could not account for the origin of the superconductivity in CsV_3Sb_5 , the spin-fluctuation mechanism seems a plausible candidate. In the theory of spin-fluctuation mediated superconductivity, the pair scattering $\Gamma_{i,j}^s(k, k')$ of a Cooper pair at \mathbf{k} to \mathbf{k}' is proportional to the RPA spin susceptibility^{39,41}, one expects that the gap function on different parts Fermi surface connected by $\mathbf{q}_1 \approx \frac{1}{4}\Gamma K$ and other sixfold-symmetric wavevectors has opposite signs, according to the linearized gap equations.

Superconductive Pairing Strengths: By solving the linearized gap equation (10), we obtain the largest singlet and triplet pairing strengths as a function of the Coulomb interaction U . The results shown in Fig. 4 indicate the singlet pairing dominates in the parameter range of U 0.6 eV. This suggests that the Cooper pairs in CsV_3Sb_5 are singlet pairing. It is consistent with the decrease of Knight shift of Sb¹⁷. Meanwhile, we find that there exists the distinct difference in the pairing strengths on the two Fermi surfaces, the pairing strength on inner Fermi surface is almost two order larger in magnitude than that on outer Fermi surface, implying the present different experimental results of one superconductive gap and two gaps are not contradictory.

The largest singlet pairing gap functions $g(k)$ at $U = 0.5$ eV and 0.8 eV are plotted in Fig. 5. These gap functions

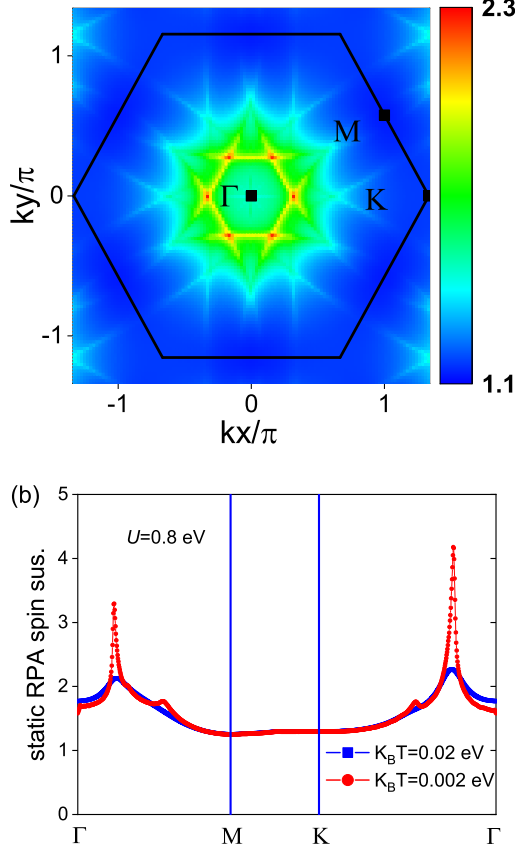


FIG. 3: (Color online) (a) Momentum-resolved spin susceptibility of pristine CsV₃Sb₅ in the first Brillouin zone for $U = 0.8$ eV, and (b) the RPA spin susceptibility along the path of high-symmetry points for different temperatures.

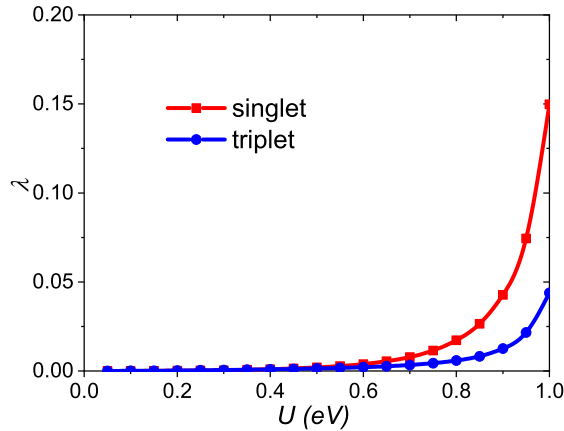


FIG. 4: (Color online) The pairing strength versus interaction U , red line for singlet channel and blue line for triplet channel, show that singlet pairing dominate the phase diagram in the range of $U > 0.4$ eV.

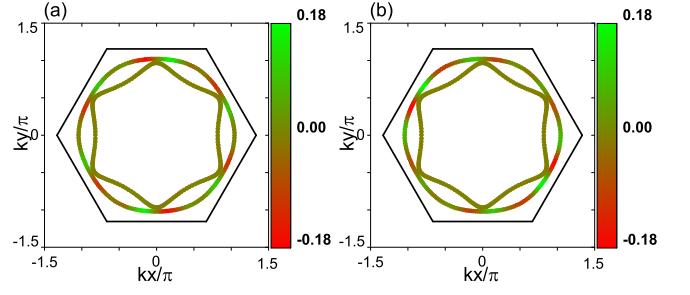


FIG. 5: The dominant singlet pairing gap function at $U = 0.5$ eV (a) and 0.8 eV (b), respectively.

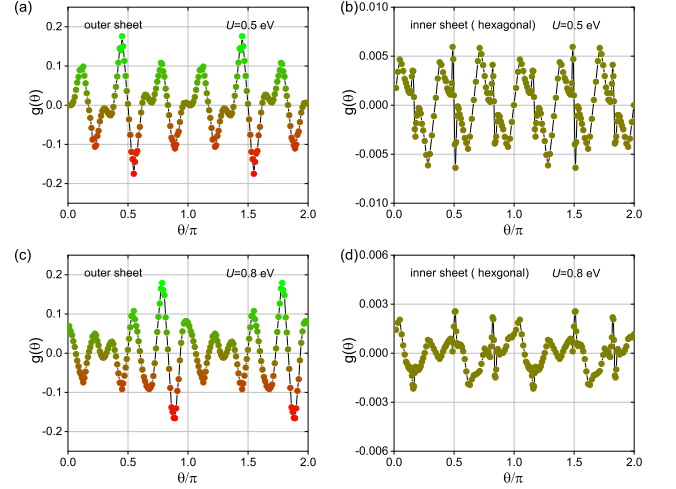


FIG. 6: The dominant singlet pairing gap function $g(k)$ versus k around Fermi surface at $U = 0.5$ eV (a),(b) and 0.8 eV (c),(d), respectively.

show sign-change at the high symmetry k points on the Fermi surface. Further analysis in Fig. 6 shows the gap function exhibiting d_{xy} -wave symmetry on the outer Fermi sheet and g-wave symmetry on the inner Fermi sheet. The gap function on the inner Fermi sheet is about smaller than that on the outer Fermi sheet by two orders of magnitude. It suggests that the d_{xy} pairing in CsV₃Sb₅. The d_{xy} wave pairing is in consistent with the results of finite linear term of thermal conductivity at ultra low temperature¹⁸ and the V-shaped gap¹⁶, which suggest the nodal superconductivity in CsV₃Sb₅. However, the study of impurity effects¹⁴ on superconductivity by STM and the appearance of Hebel-Slichter peak¹⁷ in $1/T_1T$ just below T_C proposes S-wave pairing in CsV₃Sb₅. To uncover the structure of the superconducting gap in CsV₃Sb₅, further experiments on superconducting state, such as angular-resolved photoemission spectroscopy (ARPES), Bogoliubov quasiparticle interference, and phase-sensitive tests, are crucial and highly expected.

In fitting the present effective model (1), we elaborately consider the major bands contributed from the 3d orbits of V ions and ignore the bands contributed from Sb 5p orbits.

The latter consists of the central Fermi surface around the Γ point which arises from Sb 5p orbits and a few of Fermi surface fragments arising from the hybridization between dominant Sb 5p orbits and partial V 3d orbit. One notices an experimental fact that upon applying pressure, the central Fermi surface and Sb-related 5p bands of CsV_3Sb_5 almost do not vary with the disappearance of the charge-density-wave order²⁵, while the superconducting properties change considerably with increasing pressure, suggesting that the present fitted effective minimal model is responsible for the unconventional superconductivity in CsV_3Sb_5 .

Contrast to the present singlet d_{xy} -like superconductive pairing symmetry in our effective minimal model for CsV_3Sb_5 , very recently Wu *et al.* fitted another effective 6-orbital model²⁹ based on the electronic structures of KV_3Sb_5 , they found that within the RPA their model favors the triplet f-wave pairing symmetry. This indicates that the superconductive pairing symmetry is sensitive to the details of the band structures in AV_3Sb_5 . Our present singlet pairing results agree with recent experiments, suggesting the plausible of the present effective minimal model for the superconductivity in AV_3Sb_5 .

In summary, we have obtained an effective low-energy six-band model for CsV_3Sb_5 by fitting the the first-principles elec-

tronic structures. Within the random phase approximation and on the basis of the effective minimal model, we have found that the superconducting pairing strengths increase with the lift of Coulomb correlation and decline of temperature, and superconductive pairing symmetry is singlet, most probably with the d_{xy} symmetry. These results highlight the essence of the unconventional superconductivity in Kagome compounds AV_3Sb_5 . Also, one may recall that the full effective model should include the central Fermi surface and a few of Fermi surface fragments ignored in the present study, the role of these dominant Sb 5p bands on the nature of the superconductivity in Kagome compounds AV_3Sb_5 is worthy of further investigations.

Acknowledgments

The authors thank the supports from the NSFC of China under Grant nos. 11774350 and 51727806, Program of Chinese Academy of Sciences, Science Challenge Project No. TZ2016001. Numerical calculations were partly performed at the Center for Computational Science of CASHIPS, the Sc-Grid of the Supercomputing Center, the Computer Network Information Center of CAS, the CSRC computing facility, and Hefei Advanced Computing Center.

* These authors contributed equally.

† zzeng@theory.issp.ac.cn

‡ zou@theory.issp.ac.cn

¹ Y.-M. Lu, Y. Ran, and P. A. Lee, Phys. Rev. B **83**, 224413 (2011).

² C. Chen, I. Sodemann, and P. A. Lee, Phys. Rev. B **103**, 085128 (2021).

³ B. R. Ortiz, L. C. Gomes, J. R. Morey, M. Winiarski, M. Bordelon, J. S. Mangum, I. W. H. Oswald, J. A. Rodriguez-Rivera, J. R. Neilson, S. D. Wilson, et al., Phys. Rev. Mater. **3**, 094407 (2019).

⁴ B. R. Ortiz, S. M. L. Teicher, Y. Hu, J. L. Zuo, P. M. Sarte, E. C. Schueller, A. M. M. Abeykoon, M. J. Krogstad, S. Rosenkranz, R. Osborn, et al., Phys. Rev. Lett. **125**, 247002 (2020).

⁵ Q. Yin, Z. Tu, C. Gong, Y. Fu, S. Yan, and H. Lei, Chin. Phys. Lett. **38**, 037403 (2021).

⁶ B. R. Ortiz, P. M. Sarte, E. M. Kenney, M. J. Graf, S. M. L. Teicher, R. Seshadri, and S. D. Wilson, Phys. Rev. Mater. **5**, 034801 (2021).

⁷ K. Y. Chen, N. N. Wang, Q. W. Yin, Y. H. Gu, K. Jiang, Z. J. Tu, C. S. Gong, Y. Uwatoko, J. P. Sun, H. C. Lei, et al., Phys. Rev. Lett. **126**, 247001 (2021).

⁸ Z. Zhang, Z. Chen, Y. Zhou, Y. Yuan, S. Wang, J. Wang, H. Yang, C. An, L. Zhang, X. Zhu, et al., Phys. Rev. B **103**, 224513 (2021).

⁹ X. Chen, X. Zhan, X. Wang, J. Deng, X.-B. Liu, X. Chen, J.-G. Guo, and X. Chen, Chin. Phys. Lett. **38**, 057402 (2021).

¹⁰ C. C. Zhu, X. F. Yang, W. Xia, Q. W. Yin, L. S. Wang, C. C. Zhao, D. Z. Dai, C. P. Tu, B. Q. Song, Z. C. Tao, et al., arXiv:2104.14487 (2021).

¹¹ F. H. Yu, D. H. Ma, W. Z. Zhuo, S. Q. Liu, X. K. Wen, B. Lei, J. J. Ying, and X. H. Chen, Nat. Commun. **12**, 3645 (2021).

¹² S. Ni, S. Ma, Y. Zhang, J. Yuan, H. Yang, Z. Lu, N. Wang, J. Sun, Z. Zhao, D. Li, et al., Chin. Phys. Lett. **38**, 057403 (2021).

¹³ Y. Fu, N. Zhao, Z. Chen, Q. Yin, Z. Tu, C. Gong, C. Xi, X. Zhu, Y. Sun, K. Liu, et al., Phys. Rev. Lett. **127**, 207002 (2021).

¹⁴ H.-S. Xu, Y.-J. Yan, R. Yin, W. Xia, S. Fang, Z. Chen, Y. Li, W. Yang, Y. Guo, and D.-L. Feng, Phys. Rev. Lett. **127**, 187004 (2021).

¹⁵ H. Zhao, H. Li, B. R. Ortiz, S. M. L. Teicher, P. Takamori, M. Ye, Z. Wang, B. Leon, S. D. Wilson, and Z. Ilija, Nature (London) **599**, 216 (2021).

¹⁶ H. Chen, H. Yang, B. Hu, Z. Zhao, J. Yuan, Y. Xing, G. Qian, Z. Huang, G. Li, Y. Ye, et al., Nature (London) **599**, 222 (2021).

¹⁷ C. Mu, Q. Yin, Z. Tu, C. Gong, H. Lei, Z. Li, and J. Luo, Chin. Phys. Lett. **38**, 077402 (2021).

¹⁸ C. C. Zhao, L. S. Wang, W. Xia, Q. W. Yin, J. M. Ni, Y. Y. Huang, C. P. Tu, Z. C. Tao, Z. J. Tu, C. S. Gong, et al., arXiv:2102.08356 (2021).

¹⁹ H. Tan, Y. Liu, Z. Wang, and B. Yan, Phys. Rev. Lett. **127**, 046401 (2021).

²⁰ J.-F. Zhang, K. Liu, and Z.-Y. Lu, Phys. Rev. B **104**, 195130 (2021).

²¹ W. Wu, X. Wang, and Z. Zeng, arXiv:2112.08559 (2021).

²² H. LaBollita and A. S. Botana, arXiv:2108.04876 (2021).

²³ H. Luo, Q. Gao, H. Liu, Y. Gu, D. Wu, C. Yi, J. Jia, S. Wu, X. Luo, Y. Xu, et al., arXiv:2107.02688 (2021).

²⁴ H. Li, H. Zhao, B. R. Ortiz, T. Park, M. Ye, L. Balents, Z. Wang, S. D. Wilson, and I. Zeljkovic, arXiv:2104.08209 (2021).

²⁵ Z. Liu, N. Zhao, Q. Yin, C. Gong, Z. Tu, M. Li, W. Song, Z. Liu, D. Shen, Y. Huang, et al., Phys. Rev. X **11**, 041010 (2021).

²⁶ M. Kang, S. Fang, J.-K. Kim, B. R. Ortiz, S. H. Ryu, J. Kim, J. Yoo, G. Sangiovanni, D. D. Sante, B.-G. Park, et al., arXiv:2105.01689 (2021).

²⁷ S. Cho, H. Ma, W. Xia, Y. Yang, Z. Liu, Z. Huang, Z. Jiang, X. Lu,

- J. Liu, Z. Liu, et al., arXiv:2105.05117 (2021).
- ²⁸ X. Feng, K. Jiang, Z. Wang, and J. Hu, *Sci. Bull.* **66**, 1384 (2021).
- ²⁹ X. Wu, T. Schwemmer, T. Müller, A. Consiglio, G. Sangiovanni, D. Di Sante, Y. Iqbal, W. Hanke, A. P. Schnyder, M. M. Denner, et al., *Phys. Rev. Lett.* **127**, 177001 (2021).
- ³⁰ L. Sun, X.-J. Chen, J. Guo, P. Gao, Q.-Z. Huang, H. Wang, M. Fang, X. Chen, G. Chen, Q. Wu, et al., *Nature (London)* **483**, 67 (2012).
- ³¹ P. Shahi, J. P. Sun, S. H. Wang, Y. Y. Jiao, K. Y. Chen, S. S. Sun, H. C. Lei, Y. Uwatoko, B. S. Wang, and J.-G. Cheng, *Phys. Rev. B* **97**, 020508 (2018).
- ³² E. M. Kenney, B. R. Ortiz, C. Wang, S. D. Wilson, and M. J. Graf, *J. Phys. Condens. Matter* **33**, 235801 (2021).
- ³³ S.-Y. Yang, Y. Wang, B. R. Ortiz, D. Liu, J. Gayles, E. Derunova, R. Gonzalez-Hernandez, L. Šmejkal, Y. Chen, S. S. P. Parkin, et al., *Sci. Adv.* **6**, eabb6003 (2020).
- ³⁴ I. I. Mazin and M. D. Johannes, *Nat. Phys.* **1**, 91 (2005).
- ³⁵ K. Matano, G. q. Zheng, D. Chen, C. Lin, J. Cmaidalka, R. Meng, and C. Chu, *J. Magn. Magn. Mater.* **310**, 687 (2007).
- ³⁶ T. Takimoto, T. Hotta, T. Maehira, and K. Ueda, *J. Phys. Condens. Matter* **14**, L369 (2002).
- ³⁷ T. Takimoto, T. Hotta, and K. Ueda, *J. Phys. Condens. Matter* **15**, S2087 (2003).
- ³⁸ S. Graser, T. A. Maier, P. J. Hirschfeld, and D. J. Scalapino, *New J. Phys.* **11**, 025016 (2009).
- ³⁹ D. J. Scalapino, *Rev. Mod. Phys.* **84**, 1383 (2012).
- ⁴⁰ T. Maier, T. Berlijn, and D. J. Scalapino, *Phys. Rev. B* **99**, 224515 (2019).
- ⁴¹ A. Kreisel, B. M. Andersen, P. O. Sprau, A. Kostin, J. C. S. Davis, and P. J. Hirschfeld, *Phys. Rev. B* **95**, 174504 (2017).
- ⁴² K. Kubo, *Phys. Rev. B* **75**, 224509 (2007).
- ⁴³ J. Kang, S.-L. Yu, Z.-J. Yao, and J.-X. Li, *J. Phys. Condens. Matter* **23**, 175702 (2011).
- ⁴⁴ G. Kresse and J. Furthmüller, *Phys. Rev. B* **54**, 11169 (1996).
- ⁴⁵ G. Kresse and J. Furthmüller, *Comput. Mater. Sci.* **6**, 15 (1996).
- ⁴⁶ J. P. Perdew, K. Burke, and M. Ernzerhof, *Phys. Rev. Lett.* **77**, 3865 (1996).
- ⁴⁷ A. Kokalj, *J. Mol. Graph. Model.* **17**, 176 (1999).
- ⁴⁸ G. Pizzi, V. Vitale, R. Arita, S. Blügel, F. Freimuth, G. Géranton, M. Gibertini, D. Gresch, C. Johnson, T. Koretsune, et al., *J. Phys. Condens. Matter* **32**, 165902 (2020).

